Aerospace Science and Technology 29 (2013) 92–99

Contents lists available at SciVerse ScienceDirect

Aerospace Science and Technology

www.elsevier.com/locate/aescte

Effect of swirl on the regression rate in hybrid rocket motors

C. Palani Kumar [1], Amit Kumar [*,2]

National Centre for Combustion Research and Development, Department of Aerospace Engineering, Indian Institute of Technology Madras, Chennai, Tamil Nadu-600036, India

ARTICLE INFO

Article history:
Received 7 July 2012
Received in revised form 29 January 2013
Accepted 30 January 2013
Available online 13 February 2013

Keywords:
Hybrid rocket
Regression rate
Swirl flow
Numerical simulation

ABSTRACT

In this work, the effect of swirl on regression rate (r_b) in a hybrid rocket motor is investigated numerically. The r_b increased monotonically with inlet swirl number and was also found to depend on the inlet swirl profile. The swirl velocity profiles with the peak closer to the axis yielded higher r_b. Parametric study on fuel grains of various lengths and diameters ($L/D \leqslant 25$) shows that swirl is more effective in improving the average r_b for short grains ($L/D < 5$) and large diameter grains.

1. Introduction

Hybrid rockets have many distinct advantages over conventional chemical rockets, including simplicity, fuel costs, hardware costs, and safety. However, one concern with the operation of these rockets is low r_b of the solid fuel [14,15]. While multi-port complex grain design can be used for obtaining reasonable thrust with low regression rates, this results in larger residuals and low fuel loading. Further the grain integrity also becomes a factor of concern [1].

Extensive research over the past few decades on hybrid rocket motors has contributed greatly towards the fundamental understanding of its working. One of the r_b enhancement techniques established uses swirling flow inside the combustion chamber [9,10,16,22,24]. Swirling flow in the combustion chamber can be achieved by either tangentially injecting oxidizer from the tail end [10], or using a swirl type injector [9,16,22,24] or using helical grain configuration of solid fuel [16,24].

Although r_b improvements are reported in the literature [9,10,16,22,24], the amount of swirl is most often not quantified. There is a lack of basic understanding of the effect of swirling flow on r_b of the hybrid rocket motor. The present numerical study aims to systematically understand the underlying physics and relate r_b to swirl strength, quantified by a non-dimensional swirl number.

* Corresponding author. Tel.: +91 44 22574019; fax: +91 44 22574002.
E-mail address: amitk@ae.iitm.ac.in (A. Kumar).
[1] Ph.D. Research Scholar.
[2] Associate Professor.

1270-9638/$ – see front matter
http://dx.doi.org/10.1016/j.ast.2013.01.011

2. Numerical model and solution

2.1. Geometrical configuration and computational domain

Fig. 1 presents the schematic of the hybrid rocket combustion chamber. Invariance in azimuthal direction is assumed to reduce the computational domain to a 2D axi-symmetric configuration. The shaded region in Fig. 1 is the computational domain. The domain consists of a combustion chamber and a CD nozzle. The dimensions of combustion chamber, nozzle and the details on grid are discussed later in Section 4.

2.2. Governing equations

The processes occurring inside the hybrid rocket combustion chamber can be adequately described by basic flow equations of continuity, momentum, energy and species. The governing equations in 2D cylindrical coordinates are summarized below.

Continuity equation

$$\frac{\partial}{\partial t}(\rho) + \frac{\partial}{\partial x}(\rho v_x) + \frac{\partial}{\partial r}(\rho v_r) + \frac{\rho v_r}{r} = 0 \tag{1}$$

Axial momentum equation

$$\begin{aligned}\frac{\partial}{\partial t}(\rho v_x) &+ \frac{1}{r}\frac{\partial}{\partial x}(r\rho v_x v_x) + \frac{1}{r}\frac{\partial}{\partial r}(r\rho v_r v_x) \\ &= -\frac{\partial p}{\partial x} + \frac{1}{r}\frac{\partial}{\partial x}\left[r\mu\left(2\frac{\partial v_x}{\partial x} - \frac{2}{3}(\nabla\cdot\vec{v})\right)\right] \\ &\quad + \frac{1}{r}\frac{\partial}{\partial r}\left[r\mu\left(\frac{\partial v_x}{\partial r} + \frac{\partial v_r}{\partial x}\right)\right]\end{aligned} \tag{2}$$

Nomenclature

A, A_s	Arrhenius pre-exponential factor for gas phase reaction and solid fuel pyrolysis
C	Concentration of species
C^*	Characteristic exhaust velocity .... m/s
$D_{i,m}$	Diffusivity of species i in the mixture .... m^2/s
D_i, D_0	Initial and final port diameter .... m
D_ω	Cross diffusion term
D_t	Throat diameter .... m
E_a, E_{as}	Arrhenius activation energy for gas phase reaction, solid fuel pyrolysis
$\tilde{G}_k$, G_ω	Production of k and ω
h, h_i	Sensible enthalpy of mixture and species i .... kJ/kg/s
H_R, H_P	Heat of gas phase reaction and solid fuel pyrolysis
$\vec{J}_j$	Diffusion flux of species j
k	Turbulent kinetic energy
k_r	Reaction rate constant
L	Fuel grain length .... m
p	Pressure .... N/m^2
r_b	Regression rate .... m/s
R_0	Radius of the combustion chamber .... m
R_u	Universal gas constant
Sc_t	Turbulent Schmidt number
T_s, T_∞	Surface temperature and initial temperature of fuel .... K
v_x, v_r, v_z	Axial, radial and swirl (tangential) velocity ..... m/s
W, W_i	Global reaction rate and consumption rate of species i .... $mol/m^3/s$
x, r, z	Cylindrical coordinates in axial radial and tangential direction
Y_i	Mass fraction of species i
Y_k, Y_ω	Dissipation of k and ω
α	Thermal diffusivity
Γ_k, Γ_ω	Effective diffusivities of k and ω
λ_{eff}	Effective thermal conductivity
λ_s	Thermal conductivity of the solid fuel
μ, μ_t	Molecular and turbulent viscosities .... $N\,s/m^2$
ρ	Density .... kg/m^3
ω	Specific dissipation rate

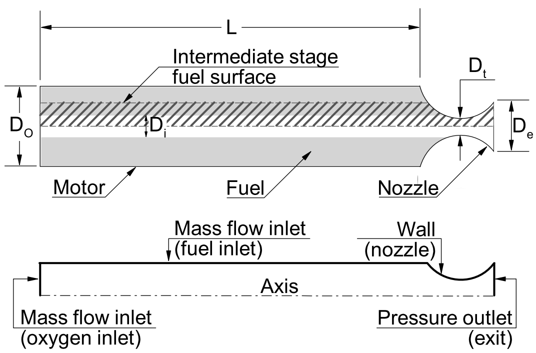

Fig. 1. Top: Schematic of a single port cylindrical hybrid rocket motor showing solid fuel grain, combustion chamber and a convergent–divergent nozzle. The shaded region is the computational domain. Bottom: Schematic of the computational domain and the boundary types.

Radial momentum equation

$$\begin{aligned}\frac{\partial}{\partial t}(\rho v_r) &+ \frac{1}{r}\frac{\partial}{\partial x}(r\rho v_x v_r) + \frac{1}{r}\frac{\partial}{\partial r}(r\rho v_r v_r)\\ &= -\frac{\partial p}{\partial r} + \frac{1}{r}\frac{\partial}{\partial x}\left[r\mu\left(\frac{\partial v_x}{\partial r} + \frac{\partial v_r}{\partial x}\right)\right]\\ &\quad + \frac{1}{r}\frac{\partial}{\partial r}\left[r\mu\left(2\frac{\partial v_r}{\partial r} - \frac{2}{3}(\nabla\cdot\vec{v})\right)\right]\\ &\quad - 2\mu\frac{v_r}{r^2} + \frac{2}{3}\frac{\mu}{r}(\nabla\cdot\vec{v}) + \rho\frac{v_z^2}{r}\end{aligned} \tag{3}$$

In the above equation the gradient of velocity vector is defined as

$$(\nabla\cdot\vec{v}) = \frac{\partial v_x}{\partial x} + \frac{\partial v_r}{\partial r} + \frac{v_r}{r} \tag{4}$$

Tangential momentum equation

$$\begin{aligned}\frac{\partial}{\partial t}(\rho v_z) &+ \frac{1}{r}\frac{\partial}{\partial x}(r\rho v_x v_z) + \frac{1}{r}\frac{\partial}{\partial r}(r\rho v_r v_z)\\ &= \frac{1}{r}\frac{\partial}{\partial x}\left[r\mu\left(\frac{\partial v_z}{\partial x}\right)\right] + \frac{1}{r^2}\frac{\partial}{\partial r}\left[r^3\mu\frac{\partial}{\partial r}\left(\frac{v_z}{r}\right)\right] - \rho\frac{v_r v_z}{r}\end{aligned} \tag{5}$$

The flow in the combustion chamber and nozzle is likely to be turbulent, therefore, an appropriate turbulence model is required. The detailed turbulence models like RSM require rigorous closure strategies and grid quality requirements and involve complexities in computation and convergence [11]. Hence these are not suited for the parametric study intended here. Simpler models like low-Re k–ε turbulence models are widely popular in literature [3–5,15]. However, under intense injection the k–ε model fails in qualitative flow prediction [26]. Although the standard k–ω model overcomes this deficiency, it is sensitive to the free stream values of ω [20]. Hence, SST k–ω model was developed [21] which combines the advantages of both k–ε (free stream accuracy) and standard k–ω (near-wall accuracy). Thus SST k–ω was used to predict turbulence in the present study.

SST *k–ω equations* are given by

$$\frac{\partial}{\partial t}(\rho k) + \frac{\partial}{\partial x_i}(\rho k u_i) = \frac{\partial}{\partial x_j}\left(\Gamma_k\frac{\partial k}{\partial x_j}\right) + \tilde{G}_k - Y_k \tag{6}$$

$$\frac{\partial}{\partial t}(\rho\omega) + \frac{\partial}{\partial x_i}(\rho\omega u_i) = \frac{\partial}{\partial x_j}\left(\Gamma_\omega\frac{\partial\omega}{\partial x_j}\right) + G_\omega - Y_\omega + D_\omega \tag{7}$$

Energy equation

$$\begin{aligned}&\frac{\partial}{\partial t}(\rho E) + \nabla\cdot\big(\vec{v}(\rho E + p)\big)\\ &\quad = \nabla\cdot\left(\lambda_{eff}\nabla T - \sum_j h_j\vec{J}_j + (\bar{\bar{\tau}}\cdot\vec{v})\right) + H_R\end{aligned} \tag{8}$$

Here E is defined as

$$E = h - \frac{p}{\rho} + \frac{v^2}{2} \tag{9}$$

Species transport equation

$$\frac{\partial}{\partial t}(\rho Y_i) + \nabla\cdot(\rho\vec{v}Y_i) = -\nabla\cdot(\vec{J}_i) + W_i \tag{10}$$

Here,

$$\vec{J}_i = -(\rho D_j + \mu_t/Sc_t)\nabla Y_j \tag{11}$$